XLVI CILAMCE
VITÓRIA - ES - BRAZIL - 2025
XLVI IBERO-LATIN AMERICAN CONGRESS ON COMPUTATIONAL METHODS IN ENGENEERING

Reliability based analysis of a railway temperature prediction model

Ary V. N. Frigeri[1], Paulo A. G. Piloto[2], Manuel Minhoto[2], Dyorgge A. Silva[1], Rubia M. Bosse[1]

[1]*Universidade Tecnológica Federal do Paraná (UTFPR)*
Av. Guarapuava, 800, 85051-010, Guarapuava-PR, Brasil
aryviniciusnf@gmail.com rubiambosse@utfpr.edu.br
[2]*GICoS, Polytechnic University of Bragança*
Campus de Santa Apolónia, 5300-253, Bragança, Portugal
ppiloto@ipb.pt mminhoto@ipb.pt

Rail temperature prediction is essential for railway safety, as extreme temperatures can lead to track buckling and structural instability. This study presents a reliability-based sensitivity analysis of a validated rail temperature model implemented in MATLAB and integrated with the UQLab framework. Two approaches were employed: a global sensitivity analysis treating all parameters as random variables, and a data-informed analysis using field measurements for key variables. The results show that ambient temperature, convection coefficient, and solar radiation are the dominant parameters affecting the output of the model. Additionally, Monte Carlo simulations were conducted using field collected weather data to estimate the daily probability of rail temperatures exceeding critical thresholds. The analysis demonstrates that these probabilities are highly sensitive to ambient temperature filtering and highlights the need for a larger scenario base to improve confidence in rare-event estimations relevant to thermal buckling.

1 Introduction

Rail temperatures play a critical role in the mechanical behavior of railway tracks. Elevated temperatures can lead to track buckling, while extremely low temperatures may cause brittle fracture. Railways are continuously exposed to varying environmental conditions—including solar radiation, wind, and seasonal temperature fluctuations—resulting in significant temperature variations along the rail profile. These temperature-induced stresses are especially relevant for Continuous Welded Rails (CWR), which, due to the absence of expansion joints, are more susceptible to thermal instabilities compared to traditional jointed tracks [1, 2].

To mitigate the risk of temperature-induced failures, various models have been developed to predict rail temperature under different weather scenarios. These models can generally be classified into two categories: empirical (statistical) models and physical models. Empirical models rely on fitted relationships derived from local data and tend to perform well within the conditions for which they were calibrated [3]. However, their applicability across different geographic regions is limited. In contrast, physical models are based on first principles of heat transfer and energy balance, allowing them to simulate rail temperature behavior under diverse and changing weather conditions. These models are particularly suitable for operational applications and risk assessments across long rail corridors and different climates [4–6].

This study focuses on the sensitivity analysis of a previously validated physical rail temperature prediction model previously proposed by Hong et al. [7] and Piloto et al. [8]. The model was implemented in MATLAB and integrated with the UQLab toolbox [9] to assess the influence of parameter uncertainties on the reliability evaluation. Key parameters such as ambient temperature, convection coefficient, and solar radiation, whose values may vary significantly depending on location, surface properties, and weather conditions, were analyzed through both global and data-informed sensitivity methods. The findings contribute to improving the robustness of temperature-based risk assessments, particularly in applications related to thermal buckling prediction and operational safety planning.

1.1 The mathematical model

This study uses a previous validated physical model that was presented by Zhang and Lee [6]. It uses a energy balance to model the temperature variation on the rail segment. This model was improved by Hong et al. [7] by

incorporating the geographical position in order to calculate the area subject to absorb the incoming solar radiation (A_s). The model demonstrates strong predictive performance, with an R^2 score ranging from 0.930 to 0.947.

Equation 1 shows such as solar radiation (*SR*), convection coefficient (h_{conv}), and various geometric and material properties. While many parameters, like air temperature (T_{air}), solar radiation, and wind velocity (w_s) are well characterized or directly measurable, others, such as the material's solar absorptivity (α_s) and emissivity (ϵ), are more challenging to determine due to their dependence on surface conditions, temperature, and wavelength. Equation 2 presents a method to calculate the convection coefficient depending on the wind speed.

$$SR \cdot \alpha_s A_s - \left[h_{conv} A_c (T_r - T_{air}) + \epsilon \sigma A_r (T_r^4 - T_{sky}^4)\right] = \rho C V \frac{dT_r}{dt}, \tag{1}$$

$$h_{conv} = \begin{cases} 5.6 + 4 \cdot w_s & ; w_s \leq 5 ms^{-1}, \\ 7.2 \cdot (w_s)^{0.78} & ; w_s > 5 ms^{-1}, \end{cases} \tag{2}$$

Where A_c is the area of rail subject to convection heat exchange, A_r is the area of the rail subject to radiation heat transfer, T_r is the rail temperature, σ is the Stefan-Boltzmann constant, T_{sky} is the atmospheric sky temperature, ρ is the density of the rail's steel, *C* is the specific heat of the rail's steel and *V* is the volume of the rail segment to be simulated.

The studies conducted by Hong et al. [7] and Piloto et al. [8] incorporate the parameter A_s (the rail profile area exposed to solar radiation) with greater detail by refining its estimation and making it dependent on both time and geographic location. In addition, the latter study released a Python package that implements the model calculations and provides a user-friendly interface for performing simulations. Figure 1 presents the validation of the *railtemp* package by comparing its results with finite element simulations conducted using ANSYS.

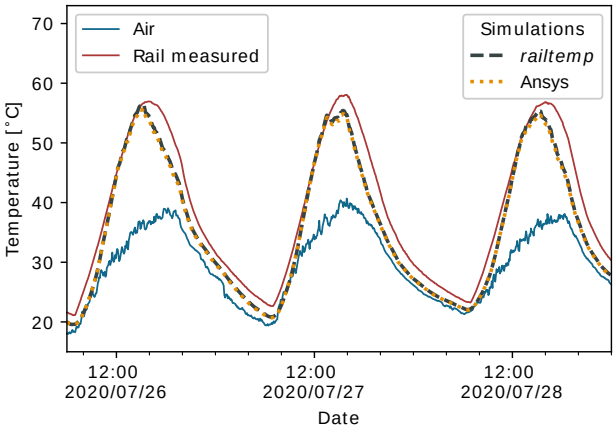


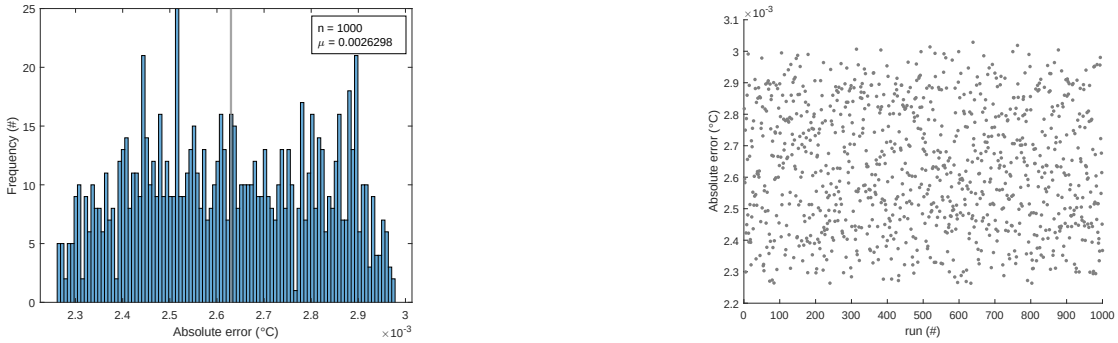
Figure 1. Validation of the railtemp package and the same solution using FEM solver from ANSYS. Adapted from Piloto et al. [8].

2 Validation of the MATLAB implementation

The Python package described in Piloto et al. [8] was implemented in MATLAB to enhance the compatibility with the UQLab [9]. Consequently, validations were performed to ensure that the Matlab simulation results matched those of the original Python package. Two types of validations were conducted: single-step and continuous.

For the single-step validation, a 300-second step interval was used, with all parameters held constant except for the initial temperature, which was randomly selected from a range of 20 °C to 50 °C. In total, 1000 simulation runs were conducted. The results are presented in Figure 2. Figure 2a illustrates that most error values fall between 2.0×10^{-3} and 3.0×10^{-3}, with an average (μ) of 2.6×10^{-3}. Additionally, Figure 2b demonstrates distribution of errors across the simulation run number highlighting a random spread of data points throughout the simulation runs.

For continuous validation, a combination of field-collected data and fixed parameters were used in the simulation, with each run spanning a total duration of 17 hours. The field-collected data included wind velocity, solar



(a) Histogram of errors.

(b) Scatter plot of aboslute errors.

Figure 2. Validation results for single step comparison.

radiation, and ambient temperature. Also, the initial temperature was randomly selected using the same range as described for the single-step validation. In total 100 simulation runs were conducted. Worth also mentioning, that for this comparison, a fixed rail area parameter for the entire simulation day was used and, for now, it does not implement the dynamic rail area described by Piloto et al. [8], since the goals was to verify the solving algorithm between *railtemp* Python package and MATLAB. The average absolute error for the continuous validation lies in a acceptable value of $4.0 \times 10^{-2}\,^{\circ}\mathrm{C}$. With this validation, we are sure that the input model to UQLab will behave extremely similar as the one from the above mentioned Python package.

3 Sensitivity analysis

Given the large number of parameters involved in the rail temperature simulation model, sensitivity analysis is essential to identify which inputs most significantly influence the model's output. In this study, a global sensitivity analysis was performed using Sobol indices, which is widely adopted for their ability to quantify the interaction (total-order) effects of input variables on output variance. These indices are based on ANOVA decomposition and assume independent input variables, with values ranging from 0 to 1, where higher values indicate greater influence. According to Cannavó [10], variables can be classified as very important ($0.8 < S_i \leq 1$), important ($0.5 < S_i \leq 0.8$), unimportant ($0.3 < S_i \leq 0.5$), and irrelevant ($0 < S_i \leq 0.3$). The sensitivity analysis was conducted in MATLAB using the UQLab package [9], in conjunction with the physical model described in Section 2.

To account for the availability of field-collected data and the fact that some parameters can be directly measured, the sensitivity analysis was structured into two main approaches. In the first approach, all model parameters were treated as random variables. This scenario, referred to as 'all parameters' involved single-step solutions with the initial rail temperature set to $30\,^{\circ}\mathrm{C}$. In the second approach, actual field measurements were incorporated for key parameters, referred to as 'w/ measured data'. Specifically, solar radiation (*SR*), wind speed (w_s), and ambient temperature (T_{air}) were set to their measured values, while the convection coefficient (h_{conv}) was calculated using equation 2 based on the measured wind speed. The sky temperature (T_{sky}) was assumed equal to the ambient temperature. All other parameters were modelled according to their respective input configurations. For this case, simulations were performed for a specific day, using measured values from 5:00 to 22:00 at five-minute intervals.

The field data used in this study was collected from a railway line in Mirandela, Portugal (latitude 41.482628, longitude -7.183741), with the rail oriented at an azimuth of $93\,\mathrm{deg}$ and a UIC54 rail profile. Further details regarding the data collection process and the railway location can be found in Piloto et al. [8].

Finally, in addition to these two analysis classes, we can split it further into: preliminary and modelled variables analysis.

3.1 Preliminary sensitivity analysis

This analysis consists on modeling all parameters with uniform random distributions, using appropriate values to the lower and upper bounds. These values were not used to describe the real probabilistic behavior of the parameter, but as an estimation to the sensitivity. Defining the random variables is discussed in the Section 3.2 The input configuration for UQLab model is described in table 1.

Table 1. Preliminary parameters distributions for UQLab.

Parameter	Type	Range	Parameter	Type	Range
α_s	Uniform	[0.1, 0.2]	ϵ	Uniform	[0.1, 1]
SR	Uniform	[0.1, 1200]	A_r	Uniform	[0.1, 1]
A_s	Uniform	[0.1, 1]	ρ	Uniform	[7840, 7860]
h_{conv}	Uniform	[0.1, 200]	***C***	Uniform	[439, 487]
A_c	Uniform	[0.1, 1]	***V***	Uniform	[0.00716, 0.00718]
T_{sky}	Uniform	[263, 333]	T_{air}	Uniform	[263, 333]

3.2 Modelling Random variables

Accurately characterizing the behavior of the model parameters is challenging without extensive experimental data under diverse conditions. Therefore, in this section, the probabilistic descriptions of the parameters are considered as approximations, informed by available literature where possible, or otherwise based on the authors' best judgment.

For the analysis where we variate all parameters, h_{conv}, $T_{air}$and *SR* are determined using field collected data and were modelled based on their best fist distribution when using all collected data for 192 days with 5 minutes interval as described by Frigeri [11, see chap. 4.1.1]. The areas subject to convection (A_c) and radiation (A_r) are modelled using half normal distribution, since it is a geometric constraint of the profile and cannot be higher than the maximum length of the profile perimeter. The area of solar absorption (A_s), on the other hand, was modelled by fitting a distribution on data calculated with the algorithm and Python package described by Piloto et al. [8] and Hong et al. [12] given the railway location as described in Section 3. The specific heat variable for the railway material (*C*) is here simplified with a uniform distribution and the range is based on the values for temperatures between $0\,^{\circ}\mathrm{C}$ to $60\,^{\circ}\mathrm{C}$ provided by Frigeri [11, see fig. 3.9b].

Zhang and Lee [6], Hong et al. [7] and Joint Commitee On Structural Safety [13] describe typical values for the solar absorption coefficient and here it is modelled using gamma distribution since by design it has bounds between 0 and 1, which is useful for coefficients of this type. Similarly, the emissivities (ϵ, ϵ_{rail} and ϵ_{amb}) values are also modelled using this type of distribution. Lastly, density and volume of the rail are modelled using normal distributions with $10\,\%$ of variation on their typical value for steel.

Table 2 shows all parameters and their modelled distributions. The notations and definitions follows the conventions in the user manual of the UQLab input module [9]. The parameter ϵ is the result distribution between other two beta distributions, namely ambient and rail emissivities. Respectively, their value are:

- ϵ_{rail}: $\mathrm{Beta}(\alpha\colon 14.7,\ \beta\colon 6.3,\ [0\ \ 1])$
- ϵ_{amb}: $\mathrm{Beta}(\alpha\colon 14.4,\ \beta\colon 9.6,\ [0\ \ 1])$

Table 2. UQlab parameters configurations defined.

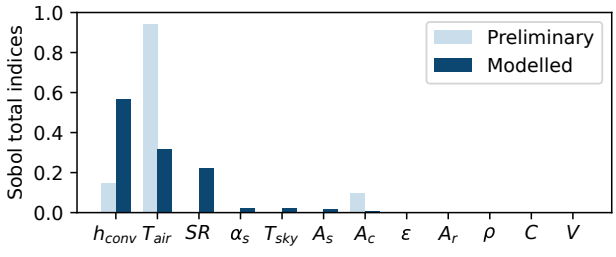
Parameter	Definition	Parameter	Definition
α_s	$\mathrm{Beta}(\alpha\colon 5.0,\ \beta\colon 2.0,\ [0\ \ 1])$	ϵ	$\mathrm{Beta}(\alpha\colon 12.0246,\ \beta\colon 16.6057,\ [0\ \ 1])$
SR	$\mathrm{Gamma}(\lambda\colon 0.0030,\ k\colon 0.9414,\ [0\ \ 1100])$	A_r	$\mathcal{N}(\mu\colon 0.43046,\ \sigma^2\colon 0.05,\ [0\ \ 0.43046])$
A_s	$\mathrm{Weibull}(a\colon 0.1540,\ b\colon 5.4147,\ [0\ \ 0.19])$	ρ	$\mathcal{N}(\mu\colon 7850,\ \sigma^2\colon 78.5)$
h_{conv}	$\mathrm{Gamma}(\lambda\colon 0.1409,\ k\colon 0.9110,\ [\ ])$	***C***	$\mathcal{U}(a\colon 439,\ b\colon 487)$
A_c	$\mathcal{N}(\mu\colon 0.43046,\ \sigma^2\colon 0.05,\ [0\ \ 0.43046])$	***V***	$\mathcal{N}(\mu\colon 7.16\times10^{-3},\ \sigma^2\colon 0.0716\times10^{-3})$
T_{sky}	$\mathcal{LN}(\lambda\colon 5.6643,\ \zeta\colon 0.0312,\ [\ ])$	T_{air}	$\mathcal{LN}(\lambda\colon 5.6643,\ \zeta\colon 0.0312,\ [\ ])$

3.3 Sensitivity analysis results

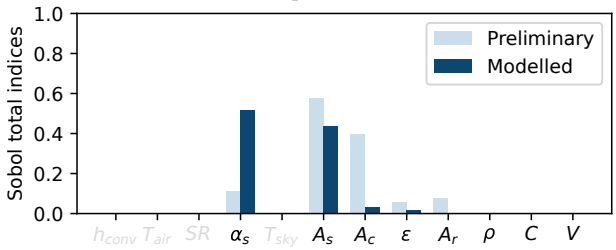
Figure 3 summarizes the total sobol index provided by the UQLab module given the inputs discussed in this section. Analyzing figure 3a it is possible to infer that the cluster of parameters that have predominance in the analysis do not substantially change between preliminary and modelled analysis. They do however have noticeable change in the index value. One can conclude that when varying and modelling all parameters of the equations,

the ones with higher impact according to the sobol index are: convection coefficient (h_{conv}), ambient temperature (T_{air}) and incoming solar radiation (*SR*). This indicates that the convection heat exchange mode has more influence (first term of eq. 1), followed by the solar radiation absorption (second term of eq. 1).

By excluding the measured parameters from the analysis (h_{conv}, T_{air}, *SR*and T_{sky}), we can estimate further the impact of the other variables in the equation. This is represented in figure 3b. We can infer that, followed by the previous mentioned terms, the other factors influencing this model are: solar absorption coefficient of the rail material (α_s), the solar absorption area (A_s) and lastly the convection exchange area (A_c). This latter analysis indicates that the second most influence heat exchange mode is by absorbing the incoming solar radiation. This also supports the fact that Hong et al. [7] and Piloto et al. [8] improve the estimation of the A_s by making it time and location dependent, since it has a high influence, when removing the measured data (mentioned in 3) from the analysis, which is in fact plausible, since these parameter are easily determined.



(a) All parameters



(b) With measured data

Figure 3. Sensitivity analysis results.

4 Monte Carlo simulations

The purpose of the Monte Carlo simulation is to offer a statistical perspective on the potential outcomes of rail temperature, considering the stochastic nature of the input parameters as defined in Section 3.2. Furthermore, this simulation technique allows us to estimate the probability that the rail temperature will reach or exceed a specific threshold. For example, in the context of buckling analysis, this phenomenon may occur when temperatures reaches or overcome the range $50\,^{\circ}\mathrm{C}$ to $60\,^{\circ}\mathrm{C}$, highly depending on the track conditions such as geometric deviation and ballast maintenance [14]. We denote these threshold probabilities as *P* values; for instance, *P60* represents the probability that the model predicts a rail temperature of $60\,^{\circ}\mathrm{C}$.

The simulations cover a single day, running from 5:00 to 22:00 with a time step of $15\,\mathrm{min}$. They utilize the field-collected data, while all other parameters are modeled as detailed in Table 2. The $A_s$parameter is here calculated directly by the *railtemp* python package. The simulation start time was chosen based on observations indicating that rail and ambient temperatures remain nearly equal during the night until early morning, allowing us to have a good guess initializing the simulation with this temperature value. For each day of available data, a total of 500 variations were generated, with data spanning 192 days. Random values for each parameter were sampled at every time step. In total, $96\,000$ simulations were executed using a cloud compute engine, supported by the Python framework *Ray* for parallel task processing. The total computational time amounted to $2\,\mathrm{h}21\,\mathrm{min}$. To streamline the configuration and execution of these simulations, the *railtemp* Python package[8] was extended with a module that accepts parameter distributions as inputs rather than fixed values. All code modifications were made publicly available in the same web repository [11, see Section 3.3.2].

To estimate the probability that the simulated rail temperature exceeds a specified threshold, (*P*) we analyze the maximum rail temperature output from each Monte Carlo simulation run. Given that T_{air} has a significant influence on the model output, as demonstrated in Section 3.3, we aggregate and calculate the *P* values conditioned on this parameter. First, the dataset is filtered to include only those simulations where the maximum ambient

temperature exceeds a defined value, $T_{\text{air}}^{\text{max}} \geq T_{\text{air}}^{\text{threshold}}$. For each simulation run i, we identify the maximum simulated rail temperature $T_{\text{rail},i}^{\text{max}}$. The probability P_T that this value exceeds a target threshold $T_{\text{rail}}^{\text{threshold}}$ is then computed as the fraction of simulation runs where the condition presented in Equation 3 is met.

$$P(T_{\text{rail}}^{\text{max}} \geq T_{\text{rail}}^{\text{threshold}} | T_{\text{air}}^{\text{max}} \geq T_{\text{air}}^{\text{threshold}}) = \frac{\text{Number of runs with } T_{\text{rail},i}^{\text{max}} > T_{\text{rail}}^{\text{threshold}}}{N}, \tag{3}$$

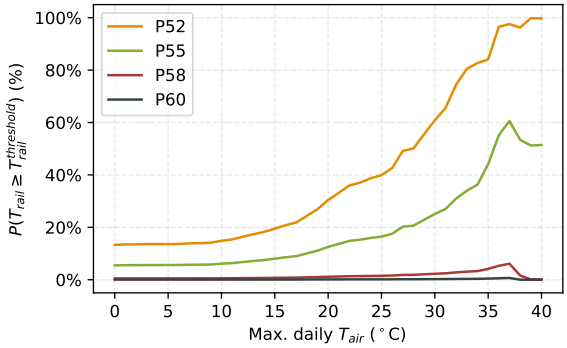
where N is the total number of simulation runs considered after filtering. Thus, P_T represents the proportion of simulations in which the rail temperature surpasses the specified threshold under the given ambient conditions.

Figure 4 shows the results of the Monte Carlo simulations, where figure 4a presents the *P* values for different rail temperatures and figure 4b shows a randomly filtered set of 1000 simulated rail temperatures (T_r) based on simulation runs for 3 consecutive days, together with the real measured rail temperature for the same period.

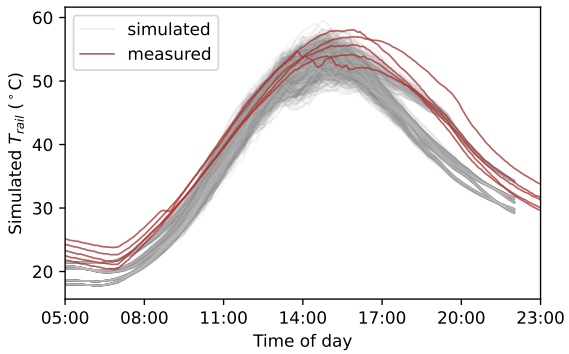
When interpreting the probabilities shown in Figure 4a, it is important to consider the number of simulation (N) available for each ambient temperature threshold ($T_{\text{air}}^{\text{threshold}}$) after the filtering. As expected, the number of days meeting the threshold condition decreases as the threshold increases. For example, for a threshold of $10\,^{\circ}\text{C}$, there are 172 days that satisfy the criterion. In contrast, only 23 days reach $35\,^{\circ}\text{C}$, 2 days reach $40\,^{\circ}\text{C}$, and no days ($N = 0$) meet or exceed $41\,^{\circ}\text{C}$. This highlights that the underlying sample size used to calculate the probabilities is not uniform across all threshold temperatures. In particular, for higher threshold values, the amount of observed and simulated data becomes limited, which affects the estimated *P* values. This limitation will be further discussed in Section 5.

With this context, *P60* reaches a maximum of $0.6\,\%$ at $37\,^{\circ}\text{C}$, corresponding to 50 simulations out of 7500, based on 15 days that met the threshold condition for filtering. These results illustrate that the *P* values vary sharply at higher T_{air} threshold levels, indicating that a greater number of simulation scenarios would be required to estimate these probabilities with higher confidence. *P55* reaches its peak value of $60\,\%$ at $38\,^{\circ}\text{C}$ (T_{air}), before decreasing to $51\,\%$ at $40\,^{\circ}\text{C}$. This highlights the influence of the number of simulations on the accuracy of the predicted probability of failure, especially in this initial stage of the study, where only experimentally measured air temperature data were used to estimate rail temperature.

Additionally, Figure 4b confirms that the input parameters leads to different simulated rail temperatures and a corresponding spread in their distribution. The figure also demonstrates that the model generally follows the measured values. Although the simulated temperatures tend to exhibit a faster decline compared to the measured data, the peak temperature values are well captured by the model.



(a) Probability of the rail temperature reaching or exceeding the threshold value, conditioned on the day's maximum ambient air temperature.



(b) Sample of 100 rail temperature simulations compared with the measured rail temperature for the same day.

Figure 4. Monte Carlo results.

5 Conclusions

The validation of the MATLAB implementation confirmed strong agreement with the original Python package, both in single-step and continuous simulations. The small absolute errors observed indicate that the reformulated solver is suitable for integration with UQLab, enabling advanced uncertainty quantification and sensitivity analysis workflows.

The sensitivity analysis revealed that ambient temperature (T_{air}), convection coefficient (h_{conv}), and solar radiation (*SR*) are the most influential parameters in the rail temperature model. When excluding directly measured

parameters, secondary factors such as the solar absorption coefficient (α_s) and radiative/convection areas (A_s, A_c) gain relevance, especially under realistic uncertainty settings.

Monte Carlo simulations demonstrated that probability estimates (*P* values) for high rail temperatures are highly sensitive to the filtering threshold of ambient temperature. For higher thresholds, the limited amount of data results in fewer scenarios available for robust estimation. For instance, the *P60* value peaked at only $0.6\,\%$, highlighting the need for additional data or synthetic weather generation to improve the confidence in rare-event risk assessments, especially in buckling-related studies.

Future work will focus on generating synthetic datasets derived from the field-collected data to expand the number of simulation scenarios and enhance the robustness of the probability estimates. In addition, narrowing the simulation time window to the critical hours—typically between 13:00 and 17:00, when $T_r$tends to peak, will enable a higher number of Monte Carlo variations within the same computational budget. This approach could also reduce dependence on field data, allowing simulations to be driven by synthetic weather profiles based on historical averages. Such a strategy would further support analyses under future climate scenarios and long-term weather trends.

Acknowledgements. The authors are thankful for the institutions that made possible this research to take place: Polytechnic Institute of Bragança (IPB); Federal University of Technology - Paraná (UTFPR); Portuguese Institute for Sea and Atmosphere (IPMA); Vale do Tua Regional Development Agency (ADRVT) and Association of Municipalities of Terra Quente Transmontana (AMTQT).

Authorship statement. The authors hereby confirm that they are the sole liable persons responsible for the authorship of this work, and that all material that has been herein included as part of the present paper is either the property (and authorship) of the authors, or has the permission of the owners to be included here.

References

[1] M. A. Van. Buckling analysis of continuous welded rail track. *Heron*, vol. 41, n. 3, pp. 175–186, 1996.

[2] A. D. Kerr. Analysis of thermal track buckling in the lateral plane. *Acta Mechanica*, vol. 30, n. 1-2, pp. 17–50, 1978.

[3] Y. Wu, P. Munro, M. G. Rasul, and M. K. M. Khan. A Review on Recent Developments in Rail Temperature Prediction for use in Buckling Studies. In *Conference on Railway Engineering*, Wellington, 2010.

[4] P. Munro. Management of track infrastructure in hot weather: a practical application, 2009.

[5] L. Chapman, J. E. Thornes, Y. Huang, X. Cai, V. L. Sanderson, and S. P. White. Modelling of rail surface temperatures: A preliminary study. *Theoretical and Applied Climatology*, vol. 92, n. 1-2, pp. 121–131. Publisher: Springer Wien, 2008.

[6] Y.-J. Zhang and S. Lee. Modeling Rail Temperature with Real-Time Weather Data. In *Transportation Research Circular*, E-C126, Indianapolis, Indiana. ISSN: 0097-8515 Issue: E-C126 Number: Weather08-001, 2008.

[7] S. U. Hong, H. U. Kim, N. H. Lim, K. H. Kim, H. Kim, and S. J. Cho. A Rail-Temperature-Prediction Model Considering Meteorological Conditions and the Position of the Sun. *International Journal of Precision Engineering and Manufacturing*, vol. 20, n. 3, pp. 337–346. Publisher: SpringerOpen, 2019.

[8] P. A. Piloto, A. V. Frigeri, M. Minhoto, and D. A. Silva. Validation of a rail temperature model with experimental measurements. *Proceedings of the Institution of Mechanical Engineers, Part F: Journal of Rail and Rapid Transit*, vol. 236, n. 9, pp. 095440972210747, 2022a.

[9] S. Marelli, C. Lamas, K. Konakli, C. Mylonas, P. Wiederkehr, and B. Sudret. UQLab user manual – Sensitivity analysis. Technical report, Chair of Risk, Safety and Uncertainty Quantification, ETH Zurich, Switzerland. Report UQLab-V2.0-106, 2022.

[10] F. Cannavó. Sensitivity analysis for volcanic source modeling quality assessment and model selection. *Computers & Geosciences*, vol. 44, pp. 52–59, 2012.

[11] A. V. N. Frigeri. Thermal and mechanical behavior of railway tracks. Master's thesis, Polytechnic Institute of Bragança, Bragança. Accepted: 2021-06-23T14:49:19Z, 2021.

[12] S. Hong, C. Park, and S. Cho. A Rail-Temperature-Prediction Model Based on Machine Learning: Warning of Train-Speed Restrictions Using Weather Forecasting. *Sensors*, vol. 21, n. 13, pp. 4606, 2021.

[13] Joint Commitee On Structural Safety. Probabilistic Model Code Part 2: Load Models. ISBN 978-3-909386-79-6, 2001.

[14] P. A. G. Piloto, A. V. N. Frigeri, and M. Minhoto. Thermal Buckling of Railways. *ce/papers*, vol. 5, n. 2, pp. 31–40. _eprint: https://onlinelibrary.wiley.com/doi/pdf/10.1002/cepa.1696, 2022b.